

# Numerical Aerodynamics Analysis of the of the Archimedes Screw Wind Turbine

Sahand Ebrahimi<sup>1</sup>, Mohammad Aref Ghassemi<sup>2</sup>

<sup>1,2</sup>Department of Maritime Engineering, Amirkabir University of Technology, Tehran, Iran

<sup>1</sup>sahand3r@aut.ac.ir

**Abstract**– Wind energy plays a key role as a sustainable source of energy and wind turbines are a relevant source of power for many countries world-wide. This paper presents the CFD based Reynolds Averaged Navier-Stocks (RANS) equation using ANSYS-CFX software. The numerical simulations for Archimedes screw wind turbine (ASWT) is performed by using the standard  $k-\omega$  SST turbulence model. The present wind turbine has three helical blades with 1.5 m in diameter. The simulation results of the pressure distribution, power coefficient and streamline velocities at various tip speed ratio (TSR) are presented and discussed.

**Keywords**– Archimedes Screw Wind Turbine, Pressure and Velocity Distribution and Power Coefficient

## I. INTRODUCTION

Wind turbines generate the green energy using the wind that causes to rotate the axis to convert the electrical energy. Wind energy is a market demand due to easy to install at rooftop of the house. Fig. 1 shows two different types of the small wind turbine installed at the rooftop of the house. The statistical official report indicates the worldwide cumulative installed wind power capacity is increasing. In 2020, it is estimated that the cumulative installed wind power capacity would reach approximately 800,000 megawatts globally. The global cumulative installed wind turbine capacity during 2001-2016 is presented in Fig. 2 [1].

There are mainly two types of the wind turbine, which can be divided into horizontal axis wind turbine (HAWT) and vertical axis wind turbine (VAWT). Both types have different configuration. More detail of the all types of the wind turbine can be found in Ref. [2].

The theory of the wind turbine and tidal turbine are something similar to the air and marine propellers. Both of them have blades and rotated around the axis. The power output of a wind turbine is dependent on the efficiency of the blades, gear assembly, alternator/dynamo, as well as wind speed and wind consistency. The power output of taller wind turbines is greater due to the fact that wind speeds are greater at higher altitudes. The power output of wind turbines can be increased by turning the head in such a way that the blades face the wind, this can be done with a wind direction sensor combined with a motorized head moving mechanism. The Yaw System is used to place the blade tips in the direction of the wind attack.

One of the advantages of ASWT is the automatically Yaw due to the Specific Shape of the blades. In fact, unlike conventional HAWTs that use Lift power, ASWT use both Lift and drag forces to rotate the blades.

The ASWT can utilize the kinetic energy from wind energy. The advantages of the ASWT will be more obvious in many circumstances, such as around buildings, because the wind turbine operates at low wind speeds. The wind direction in an urban environment changes constantly but the Archimedes wind turbine follows the wind direction automatically because the yaw is passively controlled due to the drag force. Other advantages include low noise because of the relatively low rotational speed. The disadvantage of the Archimedes wind turbine is the high thrust force compared to a propeller-type conventional HAWT [3].

In 2009, Timmer and Toet carried out fundamental research to examine the potential and optimal power output of the Archimedes spiral small wind turbine. The highest efficiency measured in their study was 12% [4].

Lu et al. developed a design method for the Archimedes spiral wind turbine blade and performed a numerical simulation [5]. Numerical study on the horizontal axis turbines arrangement in a wind farm carried out by Chen et al [6]. They showed the effect of separation distance on the turbine aerodynamic power output. Fujisawa presented the velocity measurement and numerical calculations of flow fields in and around Savonius rotors [7]. Recently, Ghassemi et al presented the hydrodynamic performance of the horizontal axis tidal stream turbine (HATST) using RANS solver [8] and also investigated the effect of the blade geometries of the HATST [9].

## II. COMPUTATIONAL SETUP

The turbulent flow around the wings was introduced as steady-state and incompressible using realizable  $k-\omega$  SST turbulent model. The ANSYS-CFX software was applied for computational fluids dynamics (CFD) simulations. The code is idealized according to the RANS Equation and Finite Volume Method of governing equations [10].

Fig. 3 shows the schematic side-view of the Archimedes Screw wind turbine blade. The pressure coefficient ( $C_{Pres}$ ), power coefficient and TSR are defined as follows:



a) Conventional wind turbine

b) ASWT

Fig. 1: Two different types of the small wind turbine installed at the rooftop of the house

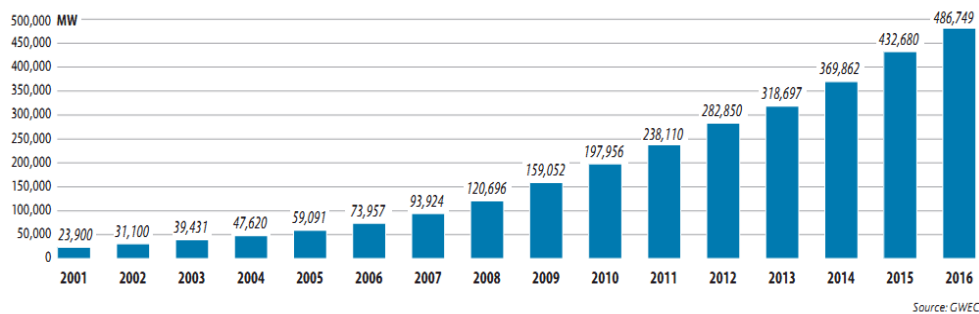


Fig. 2: Global cumulative installed wind turbine capacity 2001-2016 [1]

$$\begin{cases}
 C_p = \frac{Power}{0.5\rho U^2 RA}, & Power = Torque \times \omega \\
 C_{Pres} = \frac{P - P_{Atm}}{0.5\rho U^2}, & U^2 = V_w^2 + (2\pi rn)^2 \\
 TSR = \lambda = \frac{\omega V_{tip}}{V_w}, & \omega = 2\pi n
 \end{cases} \quad (4)$$

Where  $A$  is the platform area and  $P_{Atm}$  and  $P$  are atmosphere pressure and dynamic pressure at wing surface, respectively.  $U$  and  $V_w$  are resultant velocity and wind velocity, respectively.

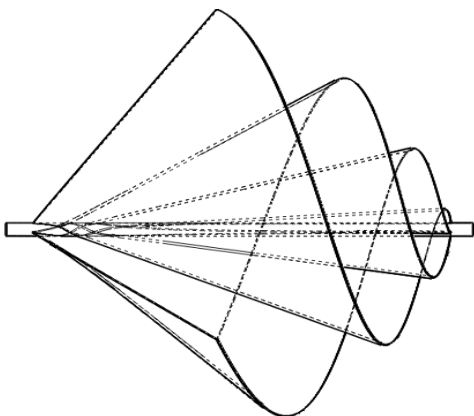


Fig. 3: Schematic of the ASWT

We selected ASWT model with 3 blades, diameter 150 mm and pitch 50 mm. Fig. 4 presents the mesh generation including the rotating domain and stationary domain. CFX separates the grid into the entire domain of using the multiple frames of reference (MFR) method, rotating domain of the spiral blade and stationary domain of the imaginary wind tunnel simulation. Two different numerical simulations were carried out. One was to predict the performance of the designed 0.5 kW Archimedes spiral wind turbine, and the other was to validate the CFD results for the 1:10 scaled down wind turbine model used for the PIV experiment. The number of cells and nodes for the real model and the scaled down model are shown separately in Table I.

Two tools of skewness and aspect ratio have been used to check the grid quality. Grid tests were performed for both cases and the grid independency was confirmed. Very fine grids were used near the turbine blade to resolve the near wake structure. The  $Y^+$  value is around less than 5 [11], [12]. Fig. 5 presents the computational domain by using MRF. The rotating domain distance from the inlet is larger than 1.5 times of the turbine diameter and the distance from the outlet is 5 times the turbine diameter. Also, the radius of the main domain is based on the minimum distance of the rotating domain to the wall, which is 1.5 times the diameter. Main domain dimensions are given on the same basis.

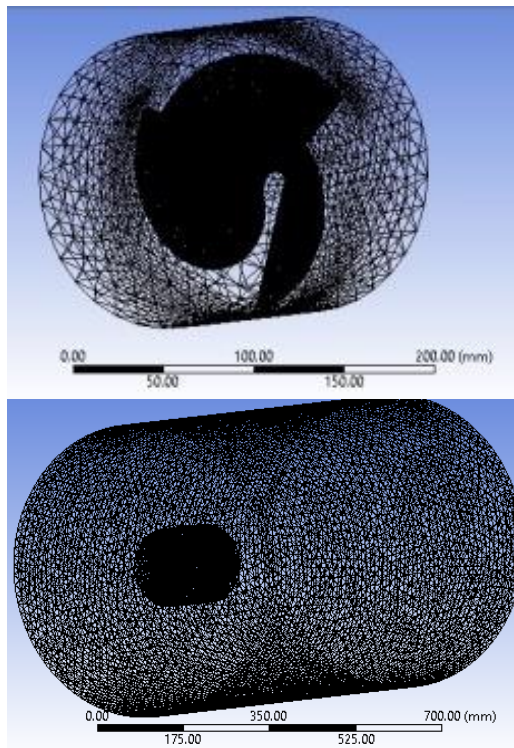


Fig. 4: Mesh generation by rotary and stationary domain

Table I: Nodes and cells number by Domain

Domain	0.5kW Class		Scaled-down	
	Nodes	Cells	Nodes	Cells
Stationary	370584	1811322	136640	729049
Rotationaly	470584	2811318	181390	966349
Total	841168	4622640	318030	1695398

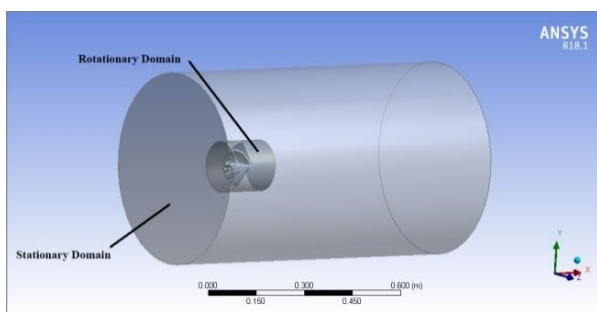


Fig. 5: Computational domain

### III. RESULTS

Here, the numerical results are presented and discussed. Fig. 6 shows pressure contour on the front and back of the blades at TSR=2.5. These images show that the pressure in front of the turbine blade (pressure side) is greater than the backs of the blades (suction side). The position of the highest and lowest pressure is on the edge of the blades.

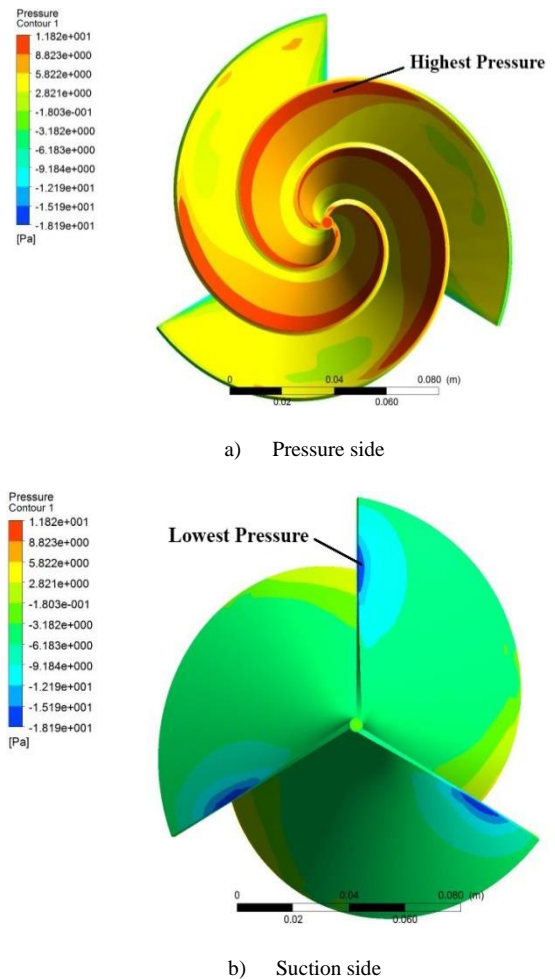


Fig. 6: Pressure contour on the blades (TSR=2.5)

When the wind flow entered to the blades, a pressure difference occurs in the front and back sides. Due to the spiral shape of the blades, the difference pressure generated force. Since the blade has helical shape (twisted shape), torque and then power is generated.

Fig. 7 shows the power coefficient ( $C_p$ ) against TSR at different speeds. The maximum power coefficient of 0.26 observed at TSR=2.5 at all speeds.

The streamline velocity is shown in Fig. 8 at two views. As can be seen, the flow velocity in the central and near the shaft reaches its lowest value. As expected, the highest flow velocity occurs in the tip region, tip speed in this region is greater than the central region. Wind flow at the tip of the blades causes torque. This event causes the turbine blades to flip in the opposite direction of flow direct.

The pressure distribution contour at TSR=2.5 is shown in Fig. 9. The flow direction is from the right to the left. As stated above, the difference in pressure between the pressure and suction sides is the blade rotational factor. When the flow rate increases, this difference in pressure also increases. The difference pressure at the tip of the blade is high, but in the central regions it is small, which means that most of the energy can be extracted from near the tip of the blade, as most HAWTs operate.

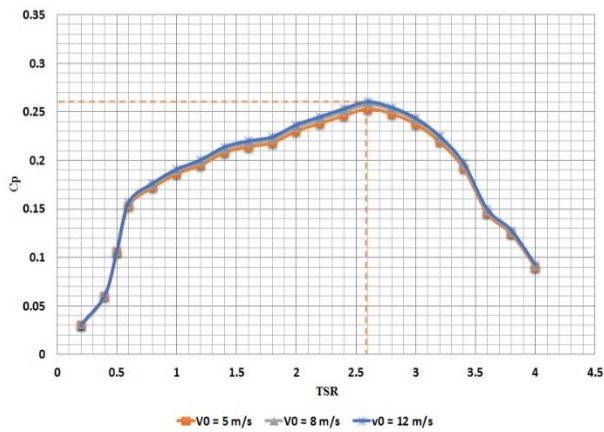


Fig. 7: Power coefficient against TSR at different speeds

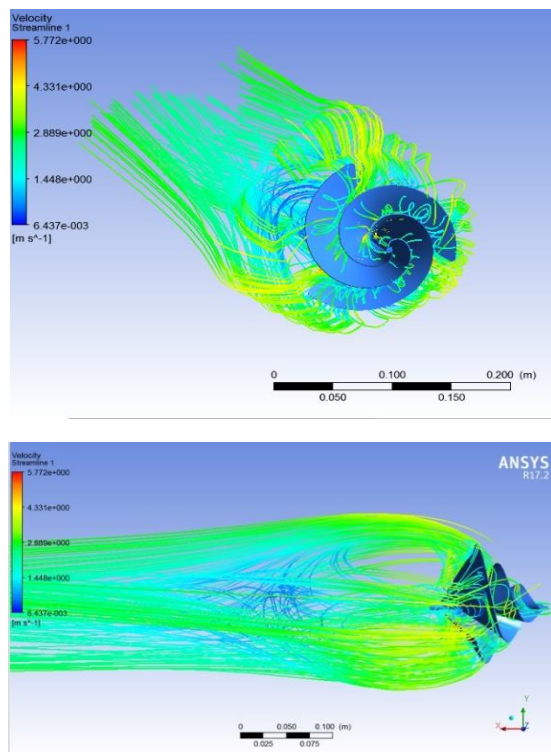


Fig. 8: Streamline velocity at different view (TSR=2.5)

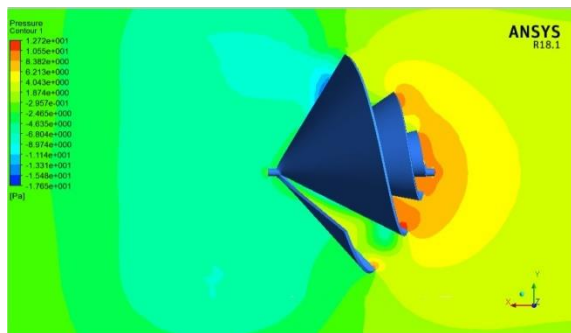


Fig. 9: Pressure contour (TSR=2.5)

#### IV. CONCLUSIONS

This paper presented the numerical results of the ASWT by using CFD solver ANSYS-CFX software. Pressure distribution streamlines velocity and power coefficient are presented and discussed. It is concluded that the maximum power coefficient is obtained 0.26 at TSR=2.5.

#### REFERENCES

- [1]. <https://www.statista.com/statistics/268363/installed-wind-power-capacity-worldwide/>
- [2]. Schaffarczyk A. P., Introduction to Wind Turbine Aerodynamics, Springer publication, 2014 (Book).
- [3]. Kim KC, Ji HS, Kim YK, Lu Q, Baek JH, Mieremet R An experimental and numerical study on aerodynamic characteristics of Archimedes spiral wind turbine blade. Energies, 2014. 7:7893–7914. doi:10.3390/en7127893
- [4]. Timmer, W.A., Toet, S. Verslag van de Metingen aan de Archimedes in de Lage-Snelheids Windtunnel van DNW; TU Delft: Delft, The Netherlands, 2009
- [5]. Lu, Q., Li, Q., Kim, Y.K.; Kim, K.C. A study on design and aerodynamic characteristics of a spiral-type wind turbine blade. J. Korean Soc. Vis. 2012, 10, 27–33.
- [6]. Choi, N.J., Nam, S.H.; Jeong, J.H.; Kim, K.C. Numerical study on the horizontal axis turbines arrangement in a wind farm: Effect of separation distance on the turbine aerodynamic power output. J. Wind Eng. Ind. Aerodyn. 2013, 117, 11–17.
- [7]. Fujisawa, N. Velocity measurement and numerical calculations of flow fields in and around Savonius rotors. J. Wind. Eng. Ind. Aerodyn. 1996, 59, 39–50.
- [8]. Abbasi A., Ghassemi H., Molyneux, D., Numerical Analysis of the Hydrodynamic Performance of HATST with Different Blade Geometries, American Journal of Civil Engineering and Architecture, 6(6), 2018, pp236--241.
- [9]. Ghassemi H, Ghafari H.R., Homayoun E., Hydrodynamic performance of the orizontal axis tidal stream turbine using RANS Solver, Scientific Journals of the Maritime University of Szczecin, 2018, 55 (127), pp23-33.
- [10]. Wilcox D., Turbulence Modeling for CFD. DCW Industries, Inc. 1994
- [11]. Lien, F.S., Yee, E., & Cheng, Y. Simulation of mean flow and turbulence over a 2D building array using high-resolution CFD and a distributed drag force approach. Journal of Wind Engineering and Industrial Aerodynamics, 92(2), 2004, 117-158.
- [12]. Porté-Agel, F., Wu, Y.T., Lu, H., Conzemius, R.J. Large-eddy simulation of atmospheric boundary layer flow through wind turbines and wind farms. J. Wind Eng. Ind. Aerodyn. 2011, 99, 154–168.